

STUDY OF SCALAR TOP QUARKS IN THE NEUTRALINO AND CHARGINO DECAY CHANNEL AT A FUTURE e^+e^- LINEAR COLLIDER

R. KERANEN, A. SOPCZAK^a
Karlsruhe University

H. NOWAK
DESY-Zeuthen

M. BERGGREN
LPNHE, Université de Paris VI & VII

The scalar top discovery potential has been studied with a full-statistics background simulation for $\sqrt{s} = 500$ GeV and $\mathcal{L} = 500$ fb⁻¹. The simulation is based on a fast and realistic simulation of a TESLA detector. The large simulated data sample allowed the application of an Iterative Discriminant Analysis (IDA) which led to a significantly higher sensitivity than in previous studies. The effects of beam polarization on signal efficiency and individual background channels are studied using separate optimization with the IDA for both polarization states. The beam polarization is very important to measure the scalar top mixing angle and to determine its mass. Simulating a 180 GeV scalar top at minimum production cross section, we obtain $\Delta m = 1$ GeV and $\Delta \cos \theta_{\tilde{t}} = 0.009$ in the neutralino decay channel, and $\Delta m = 0.5$ GeV and $\Delta \cos \theta_{\tilde{t}} = 0.004$ in the chargino decay channel.

1 Introduction

The study of the scalar top quarks is of particular interest, since the lighter stop mass eigenstate is likely to be the lightest scalar quark in a supersymmetric theory. The mass eigenstates are $m_{\tilde{t}_1}$ and $m_{\tilde{t}_2}$ with $m_{\tilde{t}_1} < m_{\tilde{t}_2}$, where $\tilde{t}_1 = \cos \theta_{\tilde{t}} \tilde{t}_L + \sin \theta_{\tilde{t}} \tilde{t}_R$ and $\tilde{t}_2 = -\sin \theta_{\tilde{t}} \tilde{t}_L + \cos \theta_{\tilde{t}} \tilde{t}_R$ with the mixing angle $\cos \theta_{\tilde{t}}$. We study the experimental possibilities to determine $m_{\tilde{t}_1}$ and $\cos \theta_{\tilde{t}}$ at a high-luminosity e^+e^- linear collider like the TESLA project¹ with the possibility of polarizing the e^- beam. The MSSM cross section was calculated with CALVIN2.0².

Previously, the discovery potential for scalar top quarks was simulated for $\sqrt{s} = 500$ GeV and $\mathcal{L} = 10$ fb⁻¹ where sequential cuts for the event selection were applied^{3,4,5}. The possibility of beam polarization to determine mass and mixing angle was studied^{6,7} and resulting estimates of the errors of the soft-breaking parameters in a supersymmetric theory were given⁸. For the neutralino decay channel the 10 fb⁻¹ study gave 4.3% signal efficiency with 21 signal and 9 background events, while in the chargino decay channel 4.5% signal efficiency with 22 signal and 8 background events were expected. These values resulted in $\Delta m = 7$ GeV and $\Delta \cos \theta_{\tilde{t}} = 0.06$.

^aandre.sopczak@cern.ch

2 Event Simulation

The simulated production process is $e^+e^- \rightarrow \tilde{t}_1 \tilde{t}_1^*$ with two decay modes:

$$1) \tilde{t}_1 \rightarrow \tilde{\chi}^0 c$$

$$2) \tilde{t}_1 \rightarrow \tilde{\chi}^+ b$$

A 100% branching fraction in each decay mode is simulated, where the $\tilde{\chi}^0$ is the Lightest Supersymmetric Particle (LSP). The first scalar top decay into a c-quark and the lightest neutralino results in a signature of two jets and large missing energy. The second investigated stop decay mode leads also to large missing energy and further jets are expected from the chargino decay. The neutralino channel is dominant unless the decay into a chargino is kinematically allowed.

The signal generator⁹ includes initial state radiation and beamstrahlung. The generated events are passed through the parametric detector simulation SGV¹⁰ tuned for a TESLA detector¹. The Simulation à Grande Vitesse (SGV) simulates colliding beam detectors in a solenoidal magnetic field. The detector geometry is described as cylinders with a common axis, parallel to the magnetic field, and as planes perpendicular to the common axis. The cylinders are described by their radius and minimum and maximum extent along this common axis. The planes are described by their position along the axis and their minimum and maximum radius. In addition, the material, the thickness in radiation lengths, and the type and precision of measurements are also given. Each cylinder or plane is divided in repeating sectors of measuring and non-measuring parts, so that blind sector-boundaries between detector sectors or over-lapping detectors are simulated. Cylindrical and plane calorimeters are specified in a similar fashion. The geometry is given in the same way, while the energy resolution and the shower axis measurement precision are given by parameters. For each charged particle generated by the bare physics simulation which is either stable or decays weakly, SGV calculates which of the tracking-detector surfaces the track helix intersects. From the list of those surfaces, the program analytically calculates the precision with which the parameters of the track can be measured. This calculation includes the multiple-scattering in the traversed surfaces, and the measurement precision at each surface that measures the track position. Each particle (neutral or charged) is also followed to its intersection with the calorimeters. The program determines which one the particle hits first (ignoring electro-magnetic calorimeters if the particle is a hadron), and using the parameters to simulate the measured energy and the direction of the shower in the detector.

For the neutralino channel we simulate a 180 GeV scalar top and a 100 GeV neutralino, and for the chargino channel a 180 GeV scalar top, a 150 GeV chargino and a 60 GeV neutralino, where the chargino decays 100% into a W boson and the neutralino. Based on experiences gained at LEP, we expect that detection efficiencies for other mass combinations are similar as long as the mass difference between the scalar top and the neutralino is larger than about 20 GeV. The relevant Standard Model background reactions, listed in Table 1, are simulated for $\mathcal{L} = 500 \text{ fb}^{-1}$.

3 Event Preselection

The event selection consists of several steps. First, an event preselection is applied using the hadronic character and large missing energy of the simulated signal. The

same preselection as for the 10 fb^{-1} study is used and we checked that similar fractions of events in each background channel pass in this 500 fb^{-1} analysis. The following preselection cuts are applied: $25 < N_{\text{cluster}} < 110$, $0.2 < E_{\text{vis}}/\sqrt{s} < 0.7$, $E_{\parallel}^{\text{imb}}/E_{\text{vis}} < 0.5$, $\text{thrust} < 0.95$, $|\cos \theta_{\text{thrust}}| < 0.7$ where N_{cluster} is the number of energy deposits, E_{vis} the total visible energy, $E_{\parallel}^{\text{imb}}$ the energy imbalance parallel to the beam axis, and $\cos \theta_{\text{thrust}}$ the angle of the event thrust with respect to the beam axis. The number of simulated events for the signal and for each background channel, as well as the remaining events after the preselection, are given in Table 1.

Table 1: Number of simulated signal and background events before and after the preselection.

| Channel | $\tilde{\chi}^0 c \tilde{\chi}^0 \bar{c}$ | $\tilde{\chi}^+ b \tilde{\chi}^- \bar{b}$ | $q\bar{q}$ | WW | $eW\nu$ | $t\bar{t}$ | ZZ | eeZ |
|-----------|---|---|------------|--------|---------|------------|------|-------|
| (in 1000) | 50 | 50 | 6250 | 3500 | 2500 | 350 | 300 | 3000 |
| Presel. | 47% | 66% | 46788 | 115243 | 252189 | 43759 | 4027 | 4069 |

4 Neutralino Channel

The reaction $e^+e^- \rightarrow \tilde{t}_1 \tilde{t}_1^* \rightarrow \tilde{\chi}^0 c \tilde{\chi}^0 \bar{c}$ has been studied. In order to separate the signal from the background, the following selection variables are defined: visible energy, number of jets, thrust value and direction, number of clusters, transverse and parallel imbalance, acoplanarity and invariant mass of two formed jets.

Figure 1 shows the simulated visible energy and transverse momentum after the preselection. Following a tighter preselection, $E_{\text{vis}}/\sqrt{s} < 0.52$ and $N_{\text{cluster}} < 80$, 278377 background events remain. Half of these events and half of the signal events are used to train the IDA¹¹. In a first step, a cut on the IDA output variable is applied, defined by a reduction in the signal of 50%. The IDA output variable and the thrust value for the remaining signal and 7265 background events are shown in Fig. 2. These events are again passed through the IDA. Figure 3 shows the IDA output variable and the resulting number of background events as a function of the signal efficiency. For 12% efficiency, 400 background events are expected.

The polarization of the e^- beam at a future linear collider offers the opportunity to enhance and suppress the left- and right-handed couplings of the scalar top signal and to determine mass and mixing angle independently. The production cross section of each background process depends differently on the polarization. It is therefore important for a high-statistics analysis to study the expected background channels individually. The expected cross sections are given in Table 2¹². The IDA analysis is repeated for -0.9 and 0.9 polarization^b in order to take into account the different composition of the background and the expected signal cross sections. Figure 4 shows the number of background events as a function of the signal efficiency for left- and right-polarization. For 12% detection efficiency, 650 background events are expected leading to $\sigma_{\text{left}} = 54.5 \pm 1.0 \text{ fb}$, and 240 background events giving $\sigma_{\text{right}} = 50.9 \pm 1.0 \text{ fb}$, where $\Delta\sigma/\sigma = \sqrt{N_{\text{signal}} + N_{\text{background}}}/N_{\text{signal}}$.

Table 2: Background cross sections (pb) from different event generators for e^- polarization.

| Pol. of e^- | $W\nu$ GRACE | WW WOPPER | $q\bar{q}$ HERWIG | $t\bar{t}$ HERWIG | ZZ COMPHEP | Zee PYTHIA |
|------------------|-----------------|--------------|----------------------|----------------------|---------------|---------------|
| -0.9 | 6.86 | 14.9 | 14.4 | 0.771 | 1.17 | — |
| 0 | 5.59 | 7.86 | 12.1 | 0.574 | 0.864 | 6.0 |
| 0.9 | 4.61 | 0.906 | 9.66 | 0.376 | 0.554 | — |

^bFor a polarization of -0.9 , 95% of the e^- are left-polarized. In the previous analyses^{6,7,8} it was assumed that only 90% of the e^- were polarized.

Figure 1: Visible energy and transverse momentum after the preselection in the neutralino decay channel.

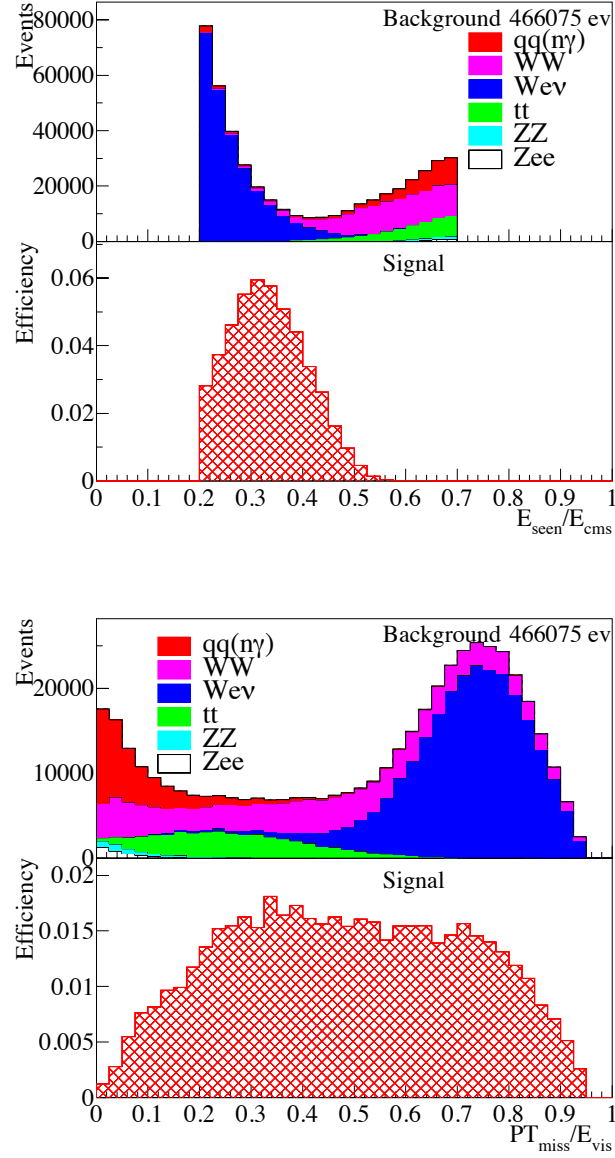


Figure 2: First step IDA output and resulting thrust values in the neutralino decay channel.

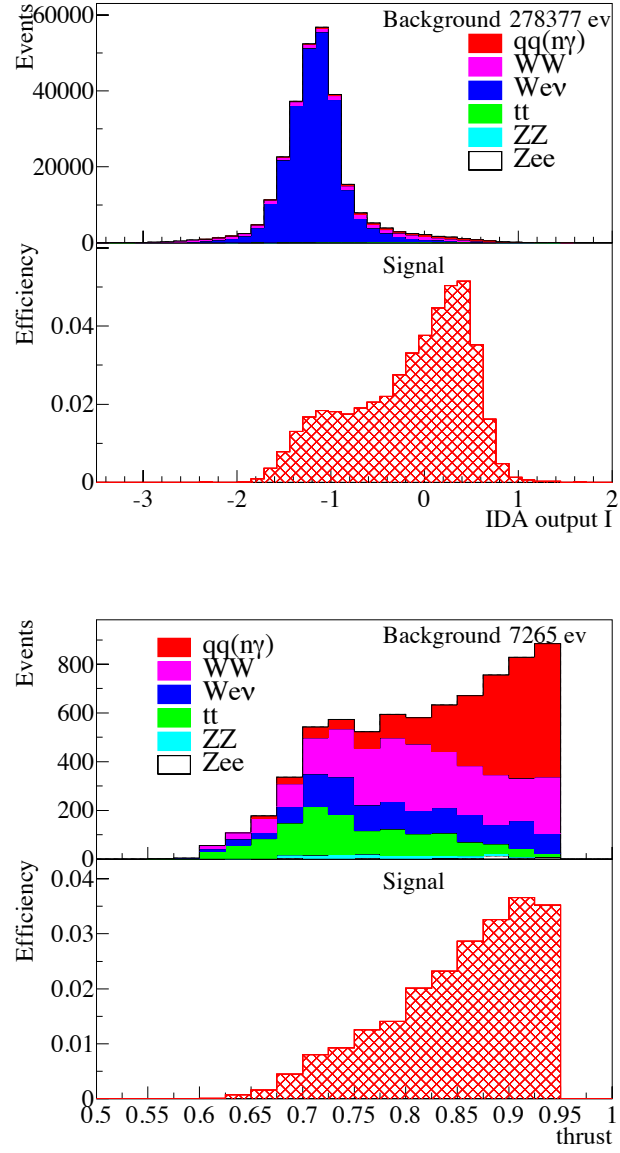


Figure 3: Final IDA output and background vs. signal efficiency in the neutralino decay channel for a 180 GeV scalar top and a 100 GeV neutralino.

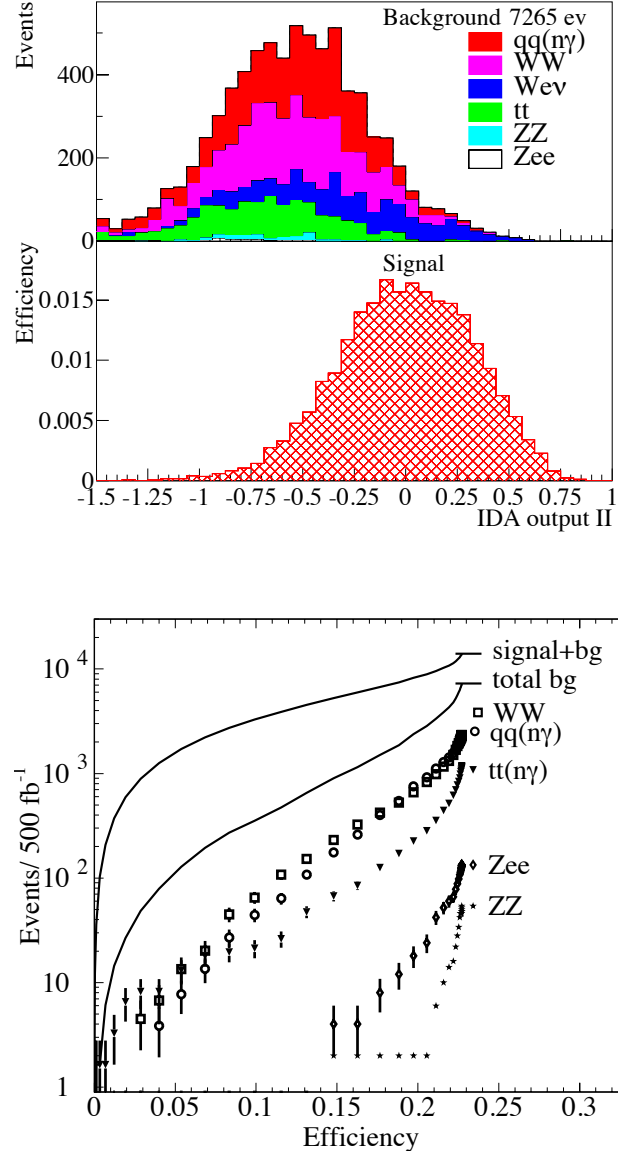
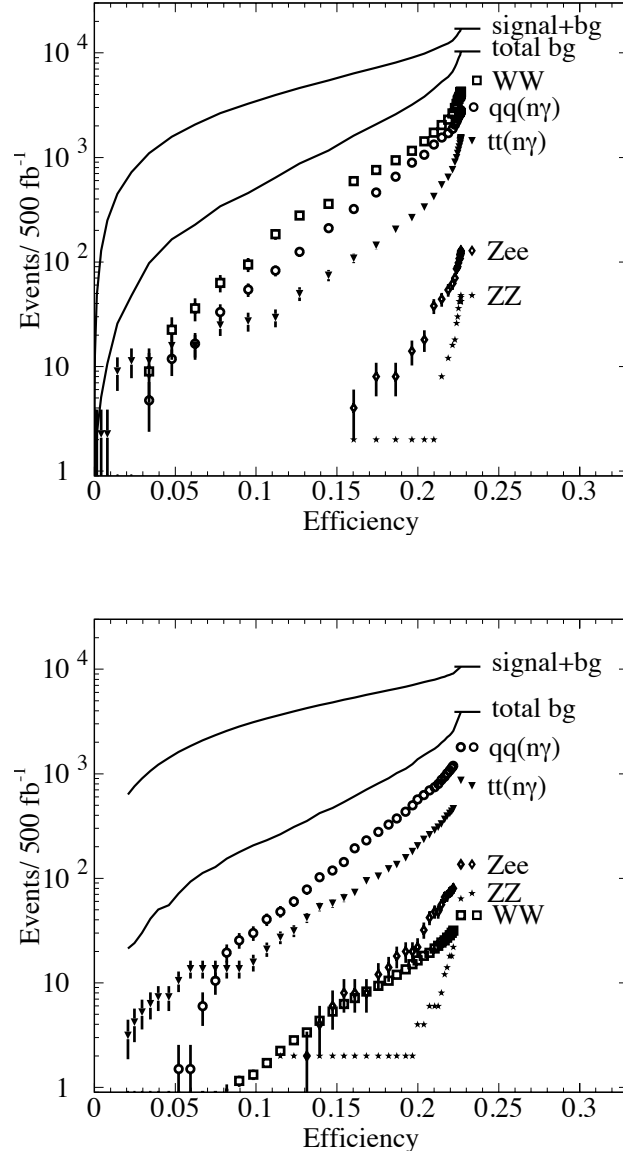


Figure 4: Background vs. signal efficiency for left- and right-polarization in the neutralino decay channel.



5 Chargino Channel

The reaction $e^+e^- \rightarrow \tilde{t}_1\tilde{t}_1^* \rightarrow \tilde{\chi}^+b\tilde{\chi}^-\bar{b} \rightarrow \tilde{\chi}^0W^+b\tilde{\chi}^0W^-\bar{b}$ has been studied with focus on the hadronic W decays. The same preselection as for the study of the neutralino channel is applied. In order to separate the signal from the background, the following selection variables are defined: visible energy, number of jets, thrust value, number of clusters, transverse and parallel imbalance, and the isolation angle of identified leptons.

Figure 5 shows the simulated visible energy and transverse momentum after the preselection. Following a tighter preselection, $E_{\text{vis}}/\sqrt{s} > 0.4$, 209051 background events remain. Half of these events and half of the signal events are used to train the IDA¹¹. In a first step, a cut on the IDA output variable is applied, defined by a reduction in the signal of 20%. The IDA output variable and the thrust value for the remaining signal and 920 background events are shown in Fig. 6. These events are again passed through the IDA. Figure 7 shows the IDA output variable and the resulting number of background events as a function of the signal efficiency. For 12% efficiency, 20 background events are expected. Allowing a background rate of 400 events as in the neutralino channel, the efficiency is 44%, from which we derive the relative error on the cross section to be 1%. In this case the number of expected signal events is much larger than the expected background, thus no separate tuning of the IDA for left- and right-polarization is required. The background is neglected for the determination of mass and mixing angle. Note that the dependence of the background rates on the polarization has to be taken into account for stop masses closer to the kinematic threshold.

6 Results

For the neutralino and chargino decay channel of scalar top quarks, we have determined the expected Standard Model background rate for a given signal efficiency. The total simulated background of about 16 million events is largely reduced, which allows a precision measurement of the scalar top production cross section with a relative error of better than 2% in the neutralino channel and about 1% in the chargino channel. Figure 8 shows the corresponding error bands and the error ellipse in the $m_{\tilde{t}_1} - \cos\theta_{\tilde{t}}$ plane for both decay channels for 90% left- and right-polarization of the e^- beam and a luminosity of 500 fb^{-1} each. The statistical errors are a factor 7 better in the neutralino channel and about a factor 14 better in the chargino channel than reported previously⁸. Based on the experience from direct searches at LEP, the systematic errors on the event selection are less than 1%, precise investigations require the detailed detector layout and a full simulation. Another uncertainty could arise from the luminosity measurement, the measurement of the polarization, and the theoretical uncertainty of the production cross section, which will be determined in the future. In conclusion, an IDA analysis based on experience at LEP2 was applied and it improved significantly the signal sensitivity. A high-luminosity linear collider with the capability of beam polarization has a great potential for precision measurements in the scalar quark sector predicted by supersymmetric theories.

Figure 5: Visible energy and transverse momentum after the preselection in the chargino decay channel.

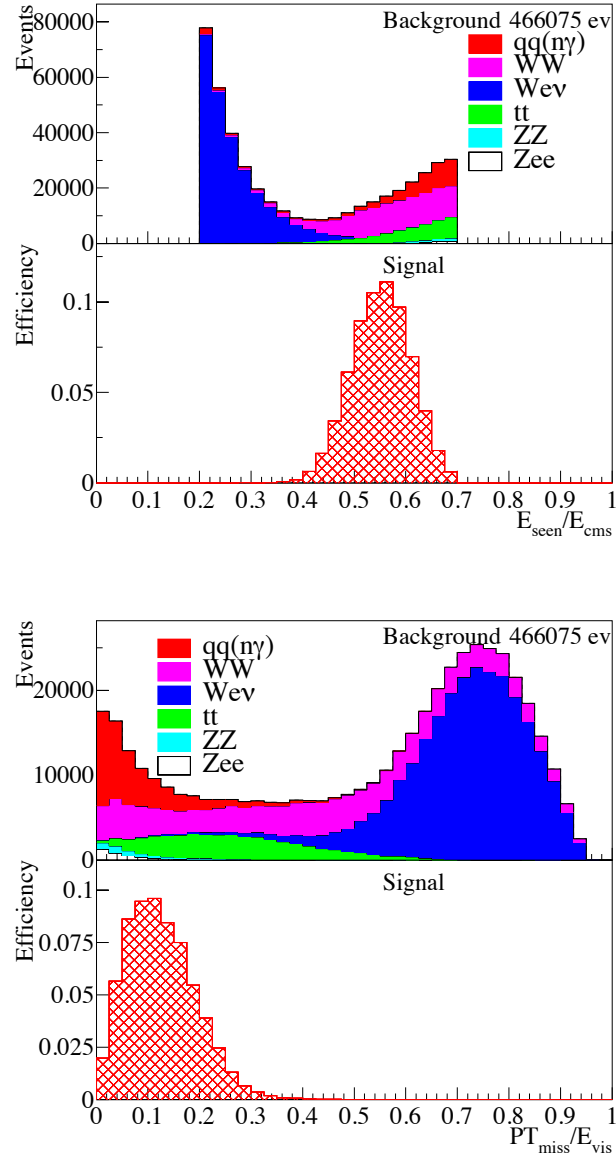


Figure 6: First step IDA output and resulting thrust values in the chargino decay channel.

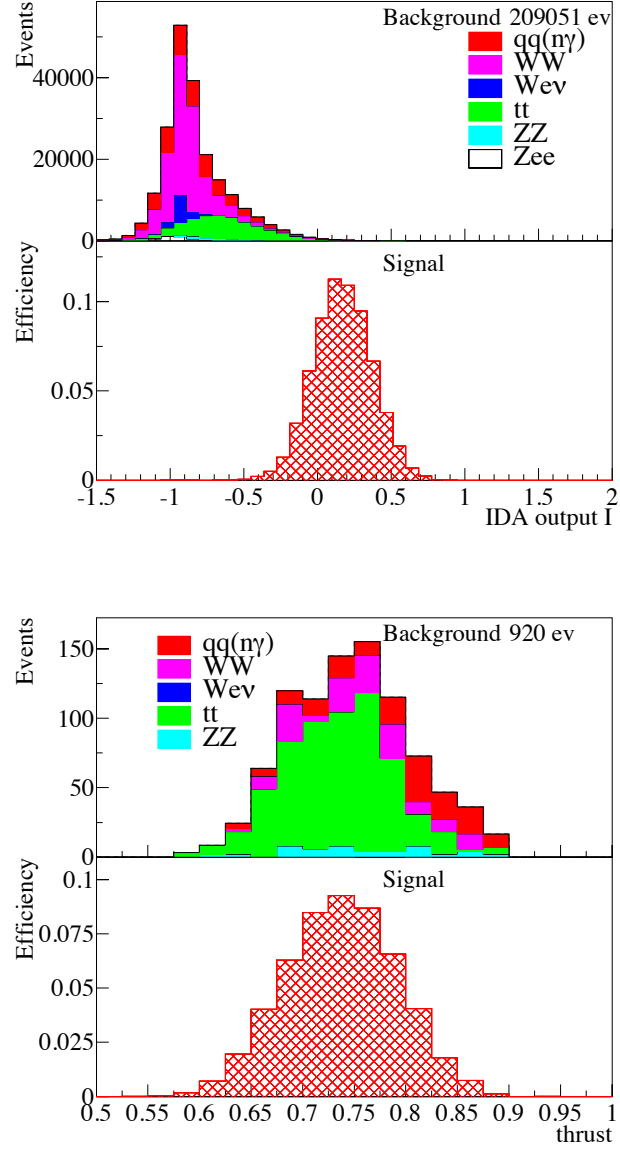


Figure 7: Final IDA output and background vs. signal efficiency in the chargino decay channel for a 180 GeV scalar top, a 150 GeV chargino and a 60 GeV neutralino.

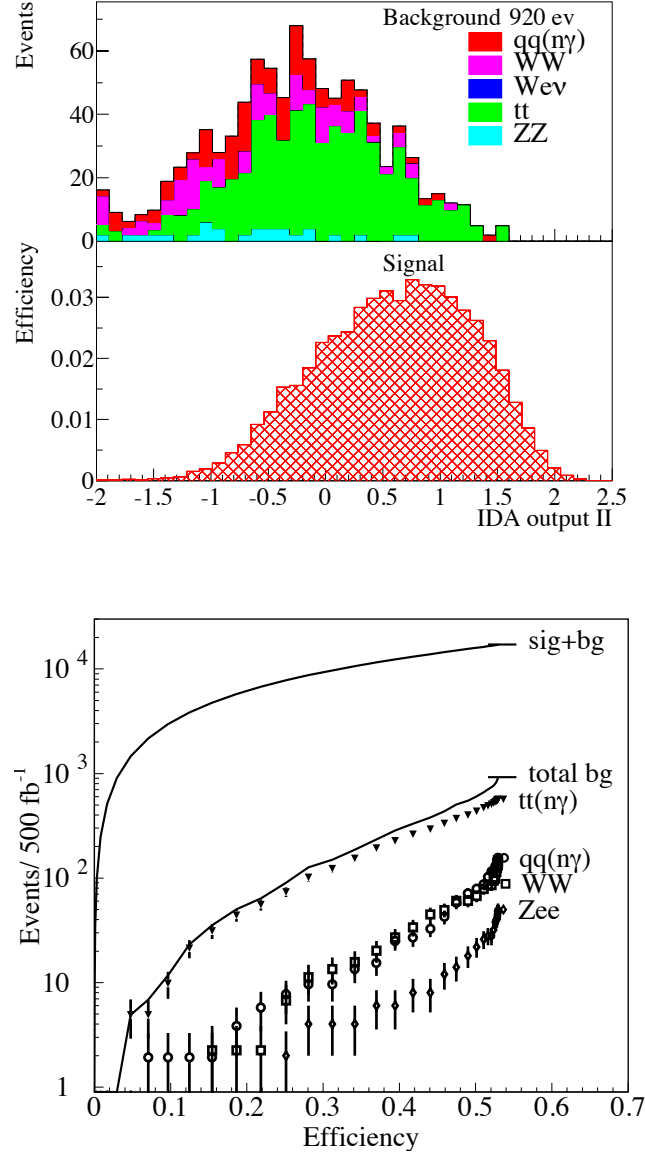
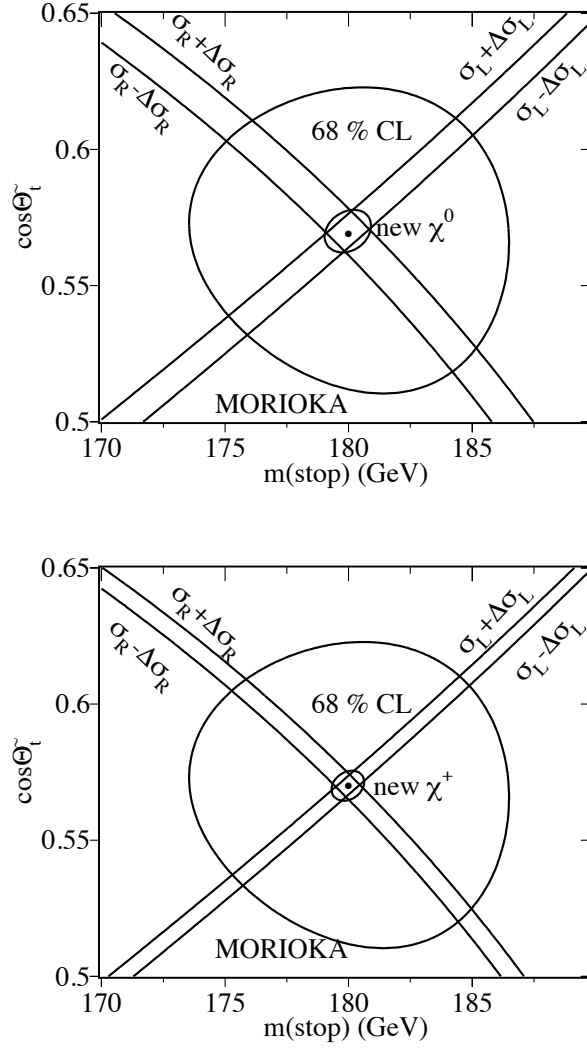


Figure 8: Error bands and the corresponding error ellipse as a function of $m_{\tilde{t}_1}$ and $\cos\theta_{\tilde{t}}$ for $\sqrt{s} = 500$ GeV and $\mathcal{L} = 500$ fb $^{-1}$. The dot corresponds to $m_{\tilde{t}_1} = 180$ GeV and $\cos\theta_{\tilde{t}} = 0.57$. The errors from the 10 fb $^{-1}$ Morioka study were $\Delta m_{\tilde{t}_1} = 7$ GeV and $\Delta\cos\theta_{\tilde{t}} = 0.06$, while the new 500 fb $^{-1}$ study gives $\Delta m_{\tilde{t}_1} = 1$ GeV and $\Delta\cos\theta_{\tilde{t}} = 0.009$ in the neutralino decay channel and $\Delta m_{\tilde{t}_1} = 0.5$ GeV and $\Delta\cos\theta_{\tilde{t}} = 0.004$ in the chargino decay channel.



References

1. ‘Conceptual Design Report of a 500 GeV e^+e^- Linear Collider with Integrated X-ray Laser Facility’, 6 DESY 1997-048, ECFA 1997-182.
2. H. Eberl, A. Bartl, W. Majerotto, *Nucl. Phys. B* **472** (1996) 481; S. Kraml, PhD thesis, hep-ph/9903257.
3. A. Sopczak, talk at the workshop ‘Physics and Experiments with Linear Colliders’, Sept. 8-12, 1995, Morioka, Japan.
4. A. Bartl et al., Proc. Morioka workshop (World Scientific) p. 571.
5. A. Bartl et al., Proc. ‘ e^+e^- Collisions at TeV Energies: The Physics Potential’, Annecy - Gran Sasso - Hamburg, 1995, DESY 96-123D, p.385.
6. A. Sopczak, talk at the workshop ‘ e^+e^- Linear Colliders: Physics and Detector Studies’, Sept. 16-17, 1996, Munich.
7. A. Bartl et al., Proc. Frascati - London - Munich - Hamburg workshop, 1996, DESY 97-123E, p. 471.
8. A. Bartl, H. Eberl, S. Kraml, W. Majerotto, W. Porod, and A. Sopczak, *Z. Phys. C* **76** (1997) 549.
9. A. Sopczak, in ‘Physics at LEP2’, CERN 96-01, p. 343.
10. M. Berggren, <http://home.cern.ch/b/berggren/www/sgv.html>
11. T.G.M. Malmgren and E.K. Johansson, *Nucl. Instr. Meth. A* **403** (1998) 481.
12. T. Sjostrand, <http://www.thep.lu.se/tf2/staff/torbjorn/LCphysgen.html>